

Oxygen Gradients in Tissue-Engineered PEGT/PBT Cartilaginous Constructs: Measurement and Modeling

J. Malda,^{1,2,3} J. Rouwkema,^{1,3} D. E. Martens,³ E. P. le Comte,⁴ F. K. Kooy,^{1,3}
J. Tramper,³ C. A. van Blitterswijk,² J. Riesle¹

¹*IsoTis S.A., P.O. Box 98, 3720 AB Bilthoven, The Netherlands;
telephone: +31 (0) 30 2295 229; fax: +31 (0) 30 2280 255;
e-mail: jos@malda.nl*

²*Institute for BioMedical Technology (BMTI), University of Twente,
The Netherlands*

³*Food and Bioprocess Engineering Group, Wageningen University,
The Netherlands*

⁴*Department of Chemical Engineering, University of Amsterdam,
The Netherlands*

Received 30 July 2003; accepted 14 November 2003

Published online 12 February 2004 in Wiley InterScience (www.interscience.wiley.com). DOI: 10.1002/bit.20038

Abstract: The supply of oxygen within three-dimensional tissue-engineered (TE) cartilage polymer constructs is mainly by diffusion. Oxygen consumption by cells results in gradients in the oxygen concentration. The aims of this study were, firstly, to identify the gradients within TE cartilage polymer constructs and, secondly, to predict the profiles during in vitro culture. A glass microelectrode system was adapted and used to penetrate cartilage and TE cartilaginous constructs, yielding reproducible measurements with high spatial resolution. Cartilage polymer constructs were cultured for up to 41 days in vitro. Oxygen concentrations, as low as 2–5%, were measured within the center of these constructs. At the beginning of in vitro culture, the oxygen gradients were steeper in TE constructs in comparison to native tissue. Nevertheless, during the course of culture, oxygen concentrations approached the values measured in native tissue. A mathematical model was developed which yields oxygen profiles within cartilage explants and TE constructs. Model input parameters were assessed, including the diffusion coefficient of cartilage (2.2×10^{-9}) + ($0.4 \times 10^{-9} \text{ m}^2 \text{ s}^{-1}$), 70% of the diffusion coefficient of water and the diffusion coefficient of constructs ($3.8 \times 10^{-10} \text{ m}^2 \text{ s}^{-1}$). The model confirmed that chondrocytes in polymer constructs cultured for 27 days have low oxygen requirements ($0.8 \times 10^{-19} \text{ mol m}^{-3} \text{ s}^{-1}$), even lower than chondrocytes in native cartilage. The ability to measure and predict local oxygen tensions offers new opportunities to obtain more insight in the relation between oxygen tension and chondrogenesis. © 2004 Wiley Periodicals, Inc.

Keywords: cartilage; tissue engineering; modeling; oxygen gradient; chondrocyte

INTRODUCTION

Articular cartilage has a limited ability to repair itself. Tissue engineering (TE) approaches may initiate functional repair and, therefore, are considered for the treatment of articular

cartilage defects. Porous scaffolds, consisting of biocompatible and biodegradable materials such as polyglycolic acid (PGA) (Freed et al., 1998, 1997; Vunjak-Novakovic et al., 1998) or polylactic acid (PLA) (Chu et al., 1995), have shown to be suitable three-dimensional carriers for seeding chondrocytes and subsequent in vitro tissue culture. Our method adopts a porous biodegradable scaffold produced from a segmented block copolymer. The segments are composed of alternating hydrophilic polyethylene glycol terephthalate (PEGT) and hydrophobic polybutylene terephthalate (PBT). By varying the ratio between these two segments, and using PEGT of different molecular weights, it is possible to control the mechanical, physicochemical, and biological properties of these copolymers (Du et al., 2002; Papadaki et al., 2001; Woodfield et al., 2002).

The natural process of articular cartilage formation and growth, chondrogenesis, is initiated by chondroprogenitor cells, which aggregate and synthesize cartilage-specific extra-cellular matrix (ECM) (Glenister, 1976). The initiation of chondrogenesis of cells seeded on three-dimensional porous scaffolds is influenced by the microenvironment of the cell. Factors, such as shear (Smith et al., 1995, 2000) the presence of growth factors (O'Driscoll, 1999; van Osch et al., 1998) and oxygen tension (Freed et al., 1998; Murphy and Sambanis, 2001b; O'Driscoll et al., 1997; Zipper et al., 1981) are thought to have a direct effect on chondrogenesis.

Previous research showed the onset of chondrogenesis within the peripheral boundaries of TE constructs (Freed et al., 1998; Obradovic et al., 2000). The absence of cartilage-specific matrix components within the middle of the TE construct at early time points could be due to inhomogeneous seeding or nutrient limitation. Due to its low solubility, oxygen is expected to be one of the first nutrients to become limiting. Apart from being an essential nutrient, oxygen is known to influence chondrocyte activity and extracellular

Correspondence to: J. Malda

matrix (ECM) production (Domm et al., 2002; Lane et al., 1977; Murphy and Sambanis, 2001a, 2001b). Within TE constructs and cartilage explants, cells consume oxygen. In a full-grown construct, convection is negligible as long as no mechanical stimulation is applied to improve the exchange of nutrients (forced convection). Therefore, the supply of oxygen within such three-dimensional structures can only take place through diffusion, which will inevitably lead to the formation of gradients in oxygen concentration. Consequently, oxygen concentrations within the cartilage can drop to 1% (Brighton and Heppenstall, 1971; Grimshaw and Mason, 2000; Silver, 1975).

The aim of the present study was to measure and model oxygen gradients within cartilaginous TE constructs during *in vitro* culture. A microelectrode suitable for cartilage was presented by Brighton et al. (Brighton and Heppenstall, 1971; Brighton et al., 1971), with which it was possible to measure the oxygen tension at cellular levels. However, due to the shape and design of the electrode, it was not possible to penetrate the tissue and measure oxygen gradients with high spatial resolution. More recently, Kellner and co-workers (2002) applied a technique for time-resolved oxygen sensing of a full-thickness construct sealed to a plate using optically sensitive foils. Although this technique is non-invasive and allows the determination of oxygen gradients with high spatial resolution, only a two-dimensional map of the oxygen profile can be obtained. For the current study, a glass microelectrode system (Revsbech and Ward, 1983) was adapted and found strong enough to penetrate cartilage and cartilage-polymer constructs, yielding reproducible measurements with high spatial resolution.

Furthermore, a mathematical model was developed to predict the oxygen profiles within the TE constructs. The straightforward model can be used in future studies to obtain more insight in the relation between the local oxygen concentration in a construct and the oxygen requirements of the cell. Moreover, this technique could also provide more insight in the relation between local oxygen tension and chondrogenesis. Other models, that predict oxygen gradients in chondrocyte containing constructs, have been described in the literature (Haselgrove et al., 1993; Nehring et al., 1999; Obradovic et al., 2000; Ye and Silverton, 1994). However, these models were never related to measured oxygen gradients, due to technical difficulties of measuring local oxygen tensions.

MATERIALS AND METHODS

Tissue Harvesting and Cell Isolation

Cartilage from the femoral condyle of 6-month-old bovine calves was harvested aseptically (1 mm³ cubes for chondrocyte isolation and \varnothing 10-mm cylindrical osteochondral explants for gradient measurements). Chondrocytes were isolated by overnight digestion with 0.15% type II collagenase (Worthington Biochemical, Lakewood, NJ). Cells

were suspended in culture medium: HEPES (Gibco-BRL, Bethesda, MD)-buffered DMEM (Gibco-BRL) supplemented with 10% FCS (Sigma-Aldrich, St. Louis, MO), 0.2 mM ascorbic acid 2-phosphate (Gibco-BRL), 0.1 mM non-essential amino acids (Sigma-Aldrich), 0.4 mM proline (Sigma-Aldrich), 100 units/ml penicillin (Gibco-BRL), and 100 μ g/mL streptomycin (Gibco-BRL).

Porous Polymer Construct Preparation

Cylindrical scaffolds (\varnothing 4 mm) were cored out of 5-mm-thick porous blocks. Porous blocks were produced by a compression moulding and salt-leaching method, as previously described (Du et al., 2002). In brief, 300PEGT55PBT45 (PolyActive[®], IsoTis S.A.) powders (PEGT/PBT ratio of 55/45 and a PEGT molecular mass of 300 g mol⁻¹) of less than 600 μ m were homogeneously mixed with sodium chloride grains. The grain size was 500–600 μ m, and the amount of the salt was adjusted to a final volume percentage of 80%. The mixture was compression moulded into a block, and then the block was immersed in demineralized water to remove sodium chloride. All the samples were steam-sterilized (15 min, 121°C) and incubated at least 1 h in culture medium prior to cell seeding.

Cell Seeding and Culture

Chondrocytes were seeded onto cylindrical scaffolds (3 million cells per scaffold) in spinner flasks agitated at 60 rpm at 37°C in humidified 5% CO₂ incubator. After 3 days, the constructs were transferred to agarose-coated six-well plates. Subsequently, the constructs were cultured on a shaker (Polymax, Heidolph Instruments, Munich, Germany) at 30 rpm in 5 mL of culture medium for up to 41 days. Culture medium was replaced every 2–3 days. Samples for histological analysis and oxygen gradient measurement were taken after 3, 14, 27, and 41 days and 14, 27, and 41 days of culture, respectively.

Measurement of Oxygen Tension

Oxygen tensions in polymer scaffolds, in cell-polymer constructs, and in osteochondral explants were measured with a glass microelectrode, which was based on an oxygen electrode originally designed by Clark and colleagues (1953), modified by Revsbech and Ward (1983) to microelectrode size. The microelectrode (tip \varnothing = 5 μ m) in combination with a micromanipulator, allows the determination of oxygen profiles with a spatial resolution of about 10 μ m (Oostra et al., 2001; Rahardjo et al., 2002). Before each measurement the electrode was calibrated using a two-point calibration with air-saturated culture medium and a saturated (anoxic) Na₂SO₃ solution. Samples were confined, preventing diffusion from the sides and the bottom, and placed in a flow cell, which was perfused with air-saturated (21% oxygen) culture medium at 37°C. After 1 h of

equilibration, the electrode was introduced up to 2,500 μm into the sample at different locations (Fig. 1, points A, B, and C). Oxygen concentration was recorded until a stable reading was obtained. Subsequently, the electrode was retracted step-wise (100 μm per step) from the sample, and the readout was registered using a computer. This procedure was repeated three times for each location.

Diffusion Coefficient

The diffusion coefficient of oxygen in the polymer was measured using the diffusion cell shown in Figure 2. The cell consists of two compartments ($V = 60 \times 10^{-6} \text{ m}^3$ each), which were kept at 37°C . The compartments were separated by the sample. The lower compartment was stirred at 1,000 rpm to ensure that the mass transfer resistance in the liquid phase was negligible. Before the start of the experiment, the lower compartment was flushed with nitrogen for deoxygenation. The upper compartment was filled with air-saturated water, and the change in oxygen concentration in the lower compartment was measured using an oxygen electrode (Yellow Springs Instruments, Yellow Springs, OH). The upper compartment was kept at 21% oxygen by continuous sparging with air, which also ensured good mixing and good mass transfer at the liquid side. The diffusion coefficient (D) was determined from the time-dependent oxygen concentration difference [Eqs. (1) and (2)] (Crank, 1975).

$$\frac{dC_{\text{lower}}(t)}{dt} = \frac{DA}{dx V_{\text{lower}}} (C_{\text{upper}} - C_{\text{lower}}(t)), \quad (1)$$

$$D = \ln \left(\frac{C_{\text{lower}}(0) - C_{\text{upper}}}{C_{\text{lower}}(t) - C_{\text{upper}}} \right) \cdot \frac{dx V_{\text{lower}}}{At}, \quad (2)$$

where t is time (s), $C_{\text{lower}}(0)$ is the oxygen concentration in the lower compartment at $t = 0$ (mol m^{-3}), C_{upper} is the oxygen concentration in the upper compartment (mol m^{-3}), $C_{\text{lower}}(t)$

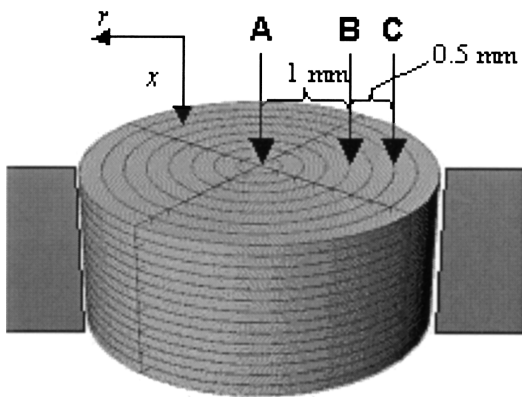


Figure 1. Schematic representation of the construct; the sample locations A, B, and C; and the subdivisions made for numerical calculations of the gradients.

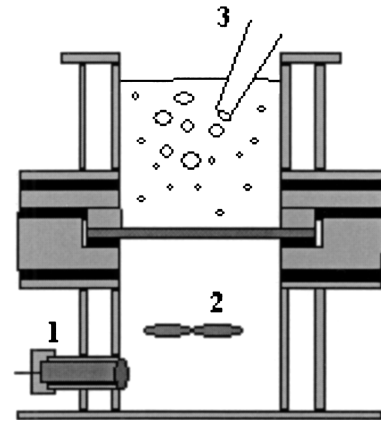


Figure 2. Schematic representation of the diffusion cell: (1) oxygen electrode; (2) stirrer; (3) aerator.

is the oxygen concentration in the lower compartment at $t = t$ (mol m^{-3}), V_{lower} is the volume of the lower compartment (m^3), A is the surface area (m^2), and dx is the thickness of the sample (m).

Cartilage slices for diffusion measurements were incubated for 24 h in 0.2% HgCl_2 (Sigma-Aldrich) in PBS in order to kill the cells and, subsequently, rinsed with PBS.

Histology

Samples were fixed using 0.14 M cacodylate buffer (pH 7.2–7.4)/1.5% glutaraldehyde, dehydrated, embedded in glycol methacrylate, and sectioned (5 μm thick). Sections were stained with haematoxylin (Sigma-Aldrich) and fast green (Merck) for cells and with safranin-O (Sigma-Aldrich) for glycosaminoglycans (GAG).

Cell Distribution Measurements

Construct samples ($n = 3$) for biochemical quantification of DNA were taken after 28 days of culture. Constructs were placed in a solution containing proteinase K (1 mg/ml), pepstatin A (10 $\mu\text{g/ml}$), and iodoacetamide (185 $\mu\text{g/ml}$) (Sigma-Aldrich) overnight at 56°C to digest the extracellular matrix (ECM) formed during culture. Quantification of total DNA was performed by Cyquant dye kit (Molecular Probes, Portland, OR) using a spectrofluorometer (Perkin-Elmer, Wellesley, MA). Total cell number per construct was obtained using a cell standard.

Spatial distributions within constructs were determined from histological sections. Cell nuclei were stained with Vectashield mounting medium containing DAPI (Vector Laboratories, Burlingame, CA). Color images ($n = 7–11$ per sample) were acquired at successive tissue depths. Images were obtained using a digital camera (Progressive 3CCD, Sony) mounted on a fluorescence microscope (E600, Nikon). DAPI staining was visualized using an XF-57 filter (Omega Optical, Brattleboro, VT). The amount of blue pixels per area was determined and assumed to be proportional

to the amount of cells in that area. Based on the geometry of the scaffold, cell distributions were calculated from the results of the image analysis and the quantitative DNA assay. Cell distributions per sample were obtained by averaging eight separate measurements.

Modeling

Equation 3 gives the oxygen concentration in a cylindrical TE construct or cartilage explant.

$$\frac{\partial C_{O_2}(x,r,t)}{\partial t} = D \left(\frac{\partial^2 C_{O_2}(x,r,t)}{\partial x^2} + \frac{\partial^2 C_{O_2}(x,r,t)}{\partial r^2} + \frac{2}{r} \frac{\partial C_{O_2}(x,r,t)}{\partial r} \right) - r_O(x,r,t), \quad (3)$$

With the following boundary conditions:

$$\begin{aligned} x = Z, \frac{\partial C(Z,r)}{\partial x} &= 0, \\ x = 0, C(0,r) &= C_{\text{medium}} (=21\%), \\ r = R, \frac{\partial C(x,R)}{\partial r} &= 0, \end{aligned}$$

where C_{O_2} is the local oxygen concentration (mol m^{-3}), x is distance (m), r is the radius (m), t is time (s), D is the diffusion coefficient of oxygen in the construct ($\text{m}^2 \text{s}^{-1}$), Z is the thickness in the x direction (m), and R is the radius of the construct (m). It was previously reported that oxygen consumption of chondrocytes follows Monod kinetics (Haselgrove et al., 1993). Thus, the oxygen consumption rate, r_O ($\text{mol m}^{-3} \text{s}^{-1}$) is given by:

$$r_O(x,r,t) = C_{\text{cell}}(x,r,t) \frac{Q_{\text{max}} C_{O_2}(x,r,t)}{K_m + C_{O_2}(x,r,t)}, \quad (4)$$

where C_{cell} is the cell density (cells m^{-3}), Q_{max} is the maximal oxygen consumption rate ($\text{mol cell}^{-1} \text{s}^{-1}$), and K_m is the oxygen concentration at half-maximal oxygen consumption (mol m^{-3}).

These equations cannot be solved using analytical methods, therefore, a numerical method was used to calculate the gradients (Appendix 1, Fig. 1).

RESULTS AND DISCUSSION

Histology

In TE constructs, cells and cell aggregates had spread throughout the whole scaffold after 3 days in culture. Nevertheless, slightly more cells were found on the outside of the constructs (Fig. 3A) as was shown for this culture method previously (Vunjak-Novakovic et al., 1998). After 14 days in vitro culture, tissue with a lacunar structure and staining intensely for GAG had formed (Fig. 3B). Constructs were covered with a dense layer of cells with a fibroblast-like appearance. After 27 days of culture, the layer of fibroblastic cells was still present and staining for GAG had slightly increased (Fig. 3C).

The average cell density, C_{cell} , at different locations at 28 days was calculated based on image analysis and DNA assay (Fig. 4). Cell densities observed decreased rapidly with depth. In contrast, in native cartilage cells are dispersed more evenly in the matrix (Hunziker et al., 2002). In addition, the cell concentration in adult hyaline cartilage [approximately $1 \times 10^7 \text{ cells cm}^{-3}$ (Hunziker et al., 2002; Stockwell, 1979)] is substantially lower than values observed in TE constructs. However, the high cell content of TE constructs, especially within the outer layers, was in line with previously reported observations by Obradovic et al. (2000).

Oxygen Measurements

Control measurements in empty porous polymer scaffolds yielded a constant output signal of 21% ($\pm 0.23\%$) oxygen equal to the signal in air-saturated culture medium (Fig. 5a). This indicates that there is no interference of the polymer with the output signal.

Oxygen concentrations within the cartilage of cylindrical osteochondral explants gradually decreased with depth and were reproducible (Fig. 5b). Relatively high concentrations of 10–12% oxygen were found at depths between 2,000 and 2,500 μm . In contrast, it has been assumed that oxygen concentrations around 1% could likely be reached (Brighton and Heppenstall, 1971; Silver, 1975). The considerably higher values reported here are probably caused by the air-saturated medium (21% oxygen) surrounding the samples

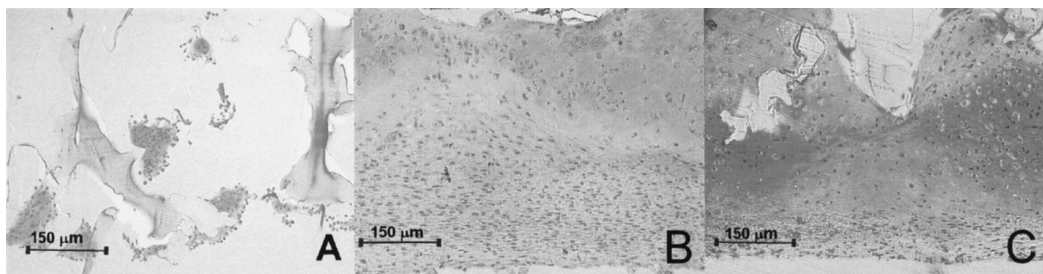


Figure 3. Photomicrographs of safranin-O stained sections of constructs cultured for 3 (A), 14 (B), and 27 (C) days. Lower parts of the pictures demonstrate the edge of the construct. A fibrous layer is had formed covering the constructs cultured for 14 (B) and 27 (C) days.

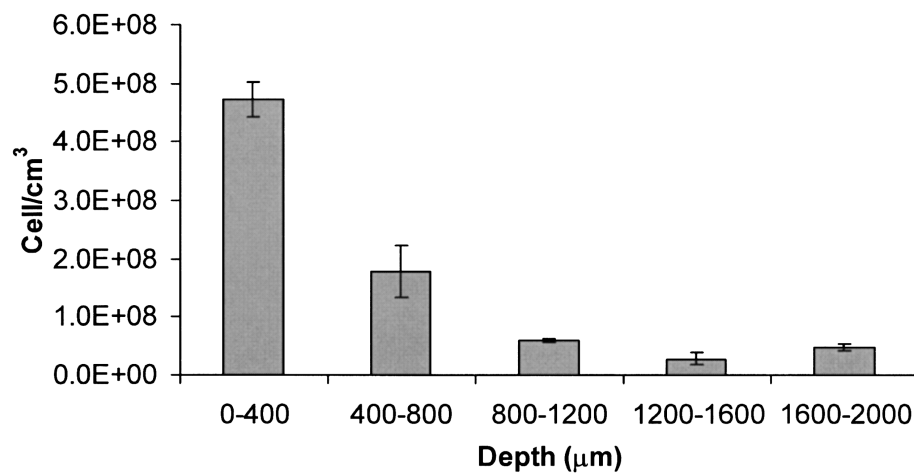


Figure 4. Cell distribution within constructs cultured for 28 days.

during the ex vivo measurements. In vivo, adult articular cartilage tissue receives its nutrients, including oxygen, from the synovial fluid by diffusion and convection caused by mechanical loading (McKibbin and Holdsworth, 1966; Stockwell, 1979). Although no data on the exact oxygen

concentration in healthy human synovial fluid is available, oxygen concentrations in the synovium will be lower than in air-saturated medium. Falchuk et al. (1970) reported oxygen concentrations as low as 7% within slightly diseased joints, whereas other authors reported slightly

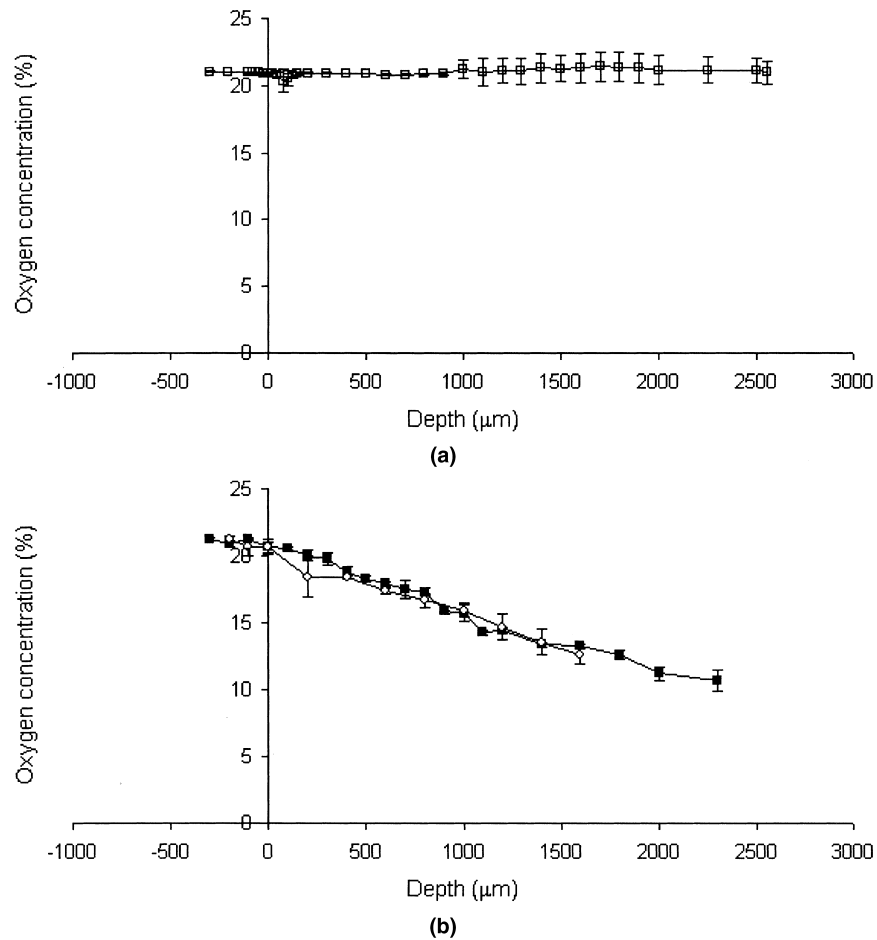


Figure 5. Oxygen concentration within a 300PEGT55PBT45 porous scaffold (a) and a vital cartilage bovine osteochondral explant (b) (two individual measurements shown).

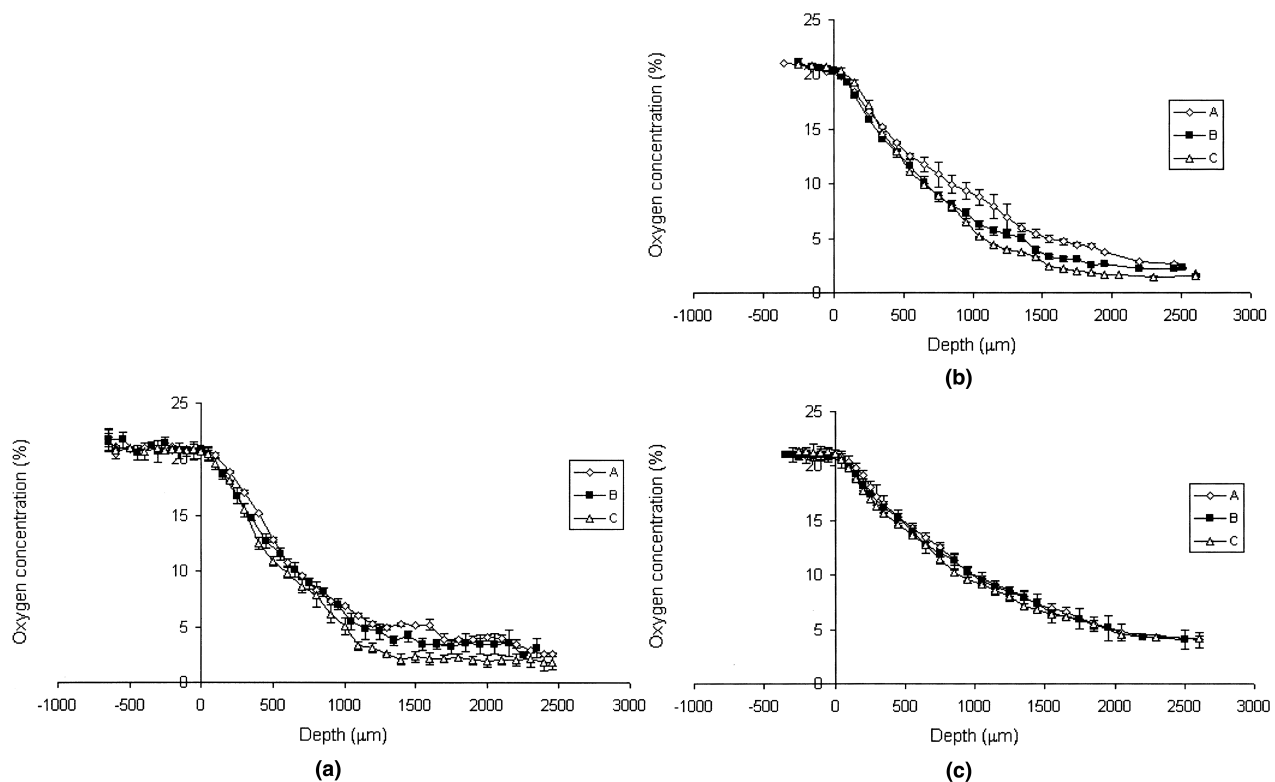


Figure 6. Oxygen concentration within cartilaginous constructs cultured for 14 (a), 27 (b), and 41 (c) days. For sample locations see Figure 1.

higher values of 10–11% (Lund-Olesen, 1970; Treuhaft and McCarty, 1971).

Oxygen gradients in TE constructs (Fig. 6a–c) were more pronounced at all time points evaluated in comparison to those measured in cartilage explants (Fig. 5b). Likely, the more rapid decrease of oxygen concentration with depth in these samples is due to the higher cellularity as well as the lower diffusion coefficient of oxygen in the constructs.

Within the center of TE constructs maintained for 14 and 27 days under aerobic conditions, oxygen concentrations, as low as 2%, were measured (Fig. 6a, b). Between the different sample locations (A, B, and C), small differences were observed. The faster decrease in oxygen tension at location C is probably caused by the higher cell concen-

tration at the outside of the constructs (Fig. 3). After 41 days of culture, oxygen measurements at three different locations were almost indistinguishable (Fig. 6c). This is in line with the more homogeneous tissue distribution throughout the whole construct as was observed in the histology pictures (data not shown).

With culture time (41 days, Fig. 6c), gradients in TE constructs became less steep, which was either caused by a decrease in cell density, a decrease in diffusion coefficient, or a decrease in the oxygen consumption rate. Recent studies demonstrated that the overall cell density does not change significantly after 28 days of in vitro culture (Malda et al., 2003). Moreover, histology revealed that the structural design of the TE construct did not significantly change during

Table I. Oxygen diffusion coefficients.

Material	D (m ² s ⁻¹)	Reference
Literature		
Water	3.0×10^{-9}	Haselgrove et al., 1993; Maroudas, 1970
Cartilage	1.5×10^{-9} (9.3×10^{-10}) – (2.5×10^{-9})	Obradovic et al., 2000 Haselgrove et al., 1993
Measured		
Bovine articular cartilage	$(2.2 \times 10^{-9}) \pm (0.4 \times 10^{-9})$	
300PEGT55PBT45	$(8.6 \times 10^{-11}) \pm (1.8 \times 10^{-11})$	
Estimated		
Cartilaginous TE construct	3.8×10^{-10}	

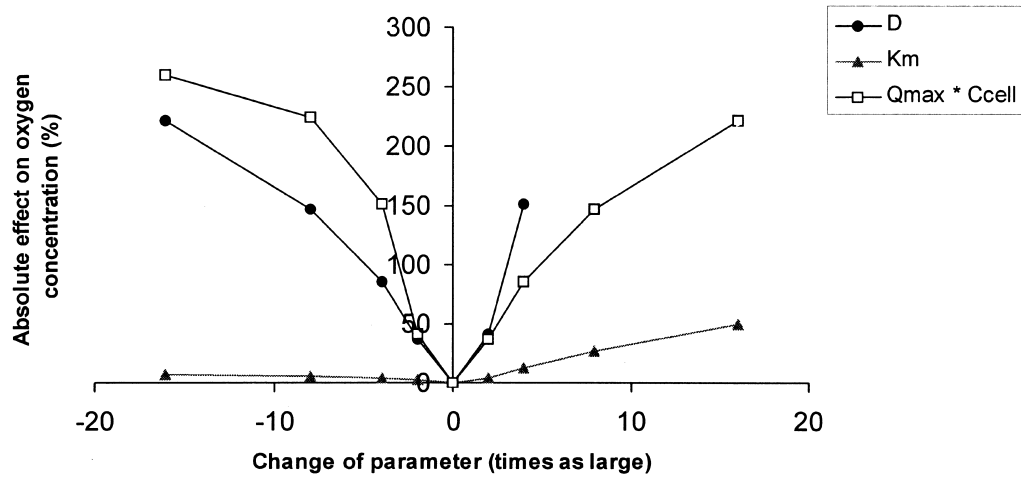


Figure 7. Sensitivity analysis of the main input parameters of the developed model, demonstrating the effect of changing one of the input parameters on the average oxygen concentration of the predicted profile.

the last 4 weeks of culture possibly be due to a low GAG synthesis rate in combination with the diffusion of GAG to the medium, as was observed previously in agitated cultures (Obradovic et al., 1999). Consequently, the oxygen diffusion coefficient will not change considerably, and the lessening of the gradient profiles is, thus, likely due to a decrease in specific oxygen consumption. Cells in the constructs gradually redifferentiate during culture from proliferating fibroblast-like cells into matrix-producing chondrogenic type, which will affect their oxygen consumption (see Modeling section).

Diffusion Coefficient Measurements

The diffusion coefficients in articular bovine cartilage and PEGT/PBT co-polymer were measured and are given in Table I. We found that the oxygen diffusion coefficient of cartilage was equal to 2.2×10^{-9} ($\pm 0.4 \times 10^{-9}$) $\text{m}^2 \text{s}^{-1}$, 71% ($\pm 13\%$) of the diffusion coefficient of water (Table I). Although the oxygen diffusion coefficient of cartilage, to the best of our knowledge, was never directly measured before, it is within the range of values assumed in several previous studies (Haselgrove et al., 1993; Obradovic et al., 2000). The diffusion coefficient of the polymer was, in contrast, approximately 25 times lower in comparison to the diffusion coefficient of native cartilage tissue. This observation stresses that the polymer is a substantial barrier for nutrients penetrating the construct and confirms the importance of the presence of interconnective pores in a scaffold for tissue-engineering purposes.

The overall diffusion coefficient of a tissue-engineered construct, D_{overall} , was estimated on the basis of the values for water (D_w), native cartilage (D_{tissue}), and the polymer (D_{polymer}) (Table I) assuming a layered structure (80% tissue and 20% polymer). The diffusion coefficient can then be calculated from $1/D_{\text{overall}} = \text{Fraction}_{\text{tissue}}/D_{\text{tissue}} + \text{Fraction}_{\text{polymer}}/D_{\text{polymer}}$. When the construct is completely filled with

tissue, the overall oxygen diffusion coefficient then equals $3.7 \times 10^{-10} \text{m}^2 \text{s}^{-1}$. In contrast, if the construct is not filled with tissue but with stagnant medium ($D_{\text{tissue}} = D_w$), the diffusion coefficient is estimated to be $3.9 \times 10^{-10} \text{m}^2 \text{s}^{-1}$. This illustrates that the diffusion coefficient of TE polymer construct mainly depends on the oxygen diffusion rate

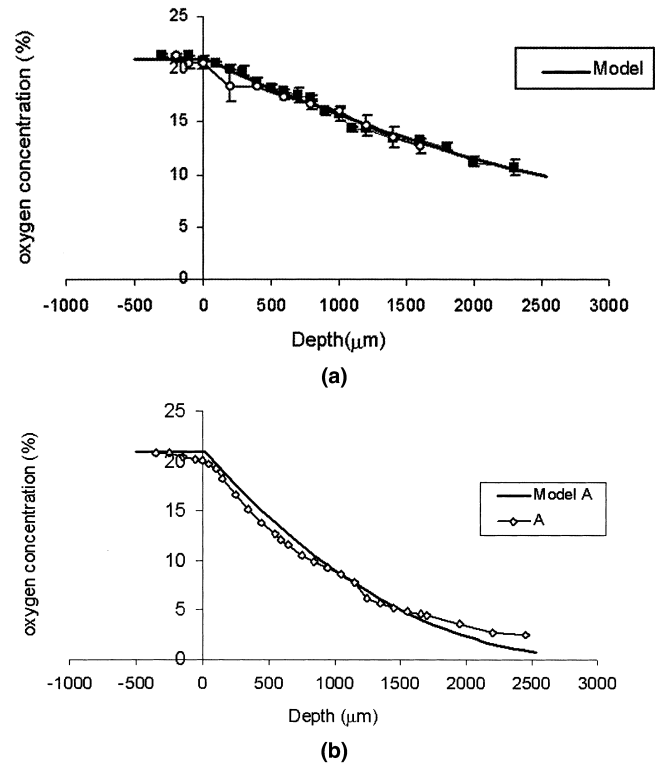


Figure 8. Model prediction and measured oxygen gradients within a vital cartilage bovine osteochondral explant (a) and a construct cultured for 27 days (b).

through the polymer. Therefore, the overall oxygen diffusion coefficient was estimated to be $3.8 \times 10^{-10} \text{ m}^2 \text{ s}^{-1}$.

Modeling

A sensitivity analysis was conducted on the main model parameters, C_{cell} , D , K_m , and Q_{max} (Fig. 7). Results are given as the absolute change in the average oxygen concentration throughout the whole construct as a function of the change in the specific parameter. Clearly the model is very sensitive to changes in C_{cell} , Q_{max} , and D , whereas the outcome of the model is less sensitive for changes in the K_m .

The model is used to describe the measured gradients in native cartilage and 27-day-old constructs. For native cartilage, the average cell density, C_{cell} , is reported to be $12 \times 10^{12} \text{ cells m}^{-3}$ for bovine cartilage (Stockwell, 1979), whereas $9.6 \times 10^{12} \text{ cells m}^{-3}$ has been reported for human cartilage (Hunziker et al., 2002). The diffusion coefficient of oxygen, D , in native cartilage was estimated by several authors (Haselgrove et al., 1993; Obradovic et al., 2000) to be in the range of 9.3×10^{-10} to $2.5 \times 10^{-9} \text{ m}^2 \text{ s}^{-1}$. In the present study, we measured a comparable value of $2.2 \times 10^{-9} \pm 0.4 \times 10^{-9} \text{ m}^2 \text{ s}^{-1}$.

Using these ranges of C_{cell} and D as the inputs for the model, combined with (the less sensitive parameter) K_m as reported by Haselgrove et al. (1993), the model was fitted to the measured gradients by varying the oxygen consumption rate, Q_{max} (Fig. 8a). Accordingly, the maximum specific oxygen consumption rate was found to be in the range of (0.2×10^{-18}) – $(4.0 \times 10^{-18}) \text{ mol cell}^{-1} \text{ s}^{-1}$. For isolated chondrocytes, Haselgrove et al. (1993) and Nehring et al. (1999) reported significantly higher values of respectively 2.0×10^{-17} and $2.78 \times 10^{-17} \text{ mol cell}^{-1} \text{ s}^{-1}$. On the other hand, it has been demonstrated (Carver and Heath, 1999; Obradovic et al., 2000) that the oxygen consumption by chondrocytes embedded in a 3D structure, such as a polymer cartilage construct, is in the range of $(2\text{--}6) \times 10^{-18} \text{ mol cell}^{-1} \text{ s}^{-1}$, which is comparable to values found here. The low respiratory activity of the chondrocytes may help them to survive in the cartilage tissue. In contrast to vascular tissues, such as muscle, where the maximal distance between oxygen supplying blood vessel and cell is in the order of 100 μm , chondrocytes do survive in blocks of tissue where the distance to the nearest blood vessel can be several millimeters or even centimeters (Stockwell, 1979).

For the TE constructs, the cell concentration as measured (Fig. 4), the estimated diffusion coefficient ($3.8 \times 10^{-10} \text{ m}^2 \text{ s}^{-1}$) of a fully grown construct and again the K_m ($5 \times 10^{-3} \text{ mol m}^{-3}$) (Haselgrove et al., 1993) were used in the model (Fig. 8b). Fitting the model to the measured oxygen gradient with a varying Q_{max} resulted in a value of $0.8 \times 10^{-19} \text{ mol m}^{-3} \text{ s}^{-1}$. This is lower than the range found for chondrocytes in native cartilage.

However, the oxygen diffusion coefficient for these constructs was estimated ($3.8 \times 10^{-10} \text{ m}^2 \text{ s}^{-1}$) based on the assumption that diffusion takes place via the shortest route possible. We are aware that the actual diffusion coefficient

could be at variance, because diffusion could take place via route of the lowest resistance. Nevertheless, preliminary data of current ongoing diffusion measurements in constructs using microelectrodes (unpublished data) yields oxygen diffusion coefficients within the same range.

CONCLUSIONS

Due to the relatively slow diffusion of oxygen through the constructs and the consumption of oxygen by cells inside the constructs, oxygen gradients occur. These gradients are even further enhanced by the regions of high cell concentrations within the peripheral boundaries of the constructs. To the best of our knowledge it was not shown previously that these gradients could be measured using a microelectrode with high spatial resolution or that these measurements could be used to verify mathematical models. We demonstrated that gradients change with culture time, and our findings suggest that cells within TE constructs adapt their metabolism and consequently have low specific oxygen consumption rates.

The ability to independently measure and model local oxygen tensions in TE cartilaginous constructs for orthopaedic surgery or in vitro evaluation offers new opportunities to obtain more insight in the behavior of chondrocytes within these constructs. Understanding of this behavior is indispensable for successful clinical implementation of TE techniques for orthopaedic reconstructive surgery.

NOMENCLATURE

A	$[\text{m}^2]$	Surface area
C_{cell}	$[\text{cells m}^{-3}]$	Cell density
C_{lower}	$[\text{mol m}^{-3}]$	Oxygen concentration in lower compartment
C_{O_2}	$[\text{mol m}^{-3}]$	Local oxygen concentration
C_{upper}	$[\text{mol m}^{-3}]$	Oxygen concentration in upper compartment
D	$[\text{m}^2 \text{ s}^{-1}]$	Diffusion coefficient
i	$[-]$	Number of layers in the x direction
j	$[-]$	Number layers r direction
K_m	$[\text{mol m}^{-3}]$	Oxygen concentration at half-maximal oxygen consumption
r	$[\text{m}]$	Radius
R	$[\text{m}]$	Radius of the construct
r_{O}	$[\text{mol m}^{-3} \text{ s}^{-1}]$	Oxygen consumption rate
Q_{max}	$[\text{mol cell}^{-1} \text{ s}^{-1}]$	Maximal oxygen consumption rate
V_{lower}	$[\text{m}^3]$	Volume of lower compartment
x	$[\text{m}]$	Distance
Z	$[\text{m}]$	Thickness in x direction

APPENDIX 1

Because Eq. (3) is not solvable using analytical methods, a numerical approach, in which the construct was divided in i layers in the vertical direction (x) and j layers in the radius direction (r), as shown in Figure 1, was used in order to describe the oxygen gradient. The radial middle layer was defined with $j = 0$, and the concentration in the outer layer was assumed to equal the concentration in the medium. Since diffusion is much faster than growth of the chondrocytes, the concentration profile will be in a pseudo

steady state on each time point. For each compartment, the following mass balance can be written:

$$\begin{aligned} V_{x,r} \frac{\Delta C_{x,r}}{\Delta t} = & A_x D \frac{C_{x-1,r} - C_{x,r}}{\Delta x} \\ & - A_x D \frac{C_{x,r} - C_{x+1}}{\Delta x} \\ & + A_{r,\text{out}} D \left(\frac{C_{x,r-1} - C_{x,r}}{\Delta r} \right) \\ & - A_{r,\text{in}} D \left(\frac{C_{x,r} - C_{x,r+1}}{\Delta r} \right) - V r_O, \end{aligned} \quad (\text{A1})$$

with

$$A_{r,\text{out}} = 2\pi\Delta x\Delta r(j+0.5), \quad (\text{A2})$$

$$A_{r,\text{in}} = 2\pi\Delta x\Delta r(j-0.5), \quad (\text{A3})$$

$$V_{x,r} = \Delta x(\pi(\Delta r(j+0.5))^2 - \pi(\Delta r(j-0.5))^2) = 2\pi k\Delta r^2\Delta x, \quad (\text{A4})$$

$$A_x = 2\pi r\Delta r. \quad (\text{A5})$$

Eq. (4) can then be written as:

$$\begin{aligned} \frac{\Delta C_{x,r}}{\Delta t} = & D \left(\frac{C_{x+1,r} - 2C_{x,r} + C_{x-1,r}}{\Delta x} \right) \\ & + D \left(\frac{(r-0.5)C_{x,r-1} - 2rC_{x,r} + (r+0.5)C_{x,r+1}}{r\Delta r^2} \right) \\ & - r_O. \end{aligned} \quad (\text{A6})$$

For the innermost cylinder the result is slightly different:

$$\begin{aligned} \frac{\Delta C_{x,0}}{\Delta t} = & D \left(\frac{C_{x+1,0} - 2C_{x,0} + C_{x-1,0}}{\Delta x} \right) \\ & - 4D \left(\frac{C_{x,0} - C_{x,1}}{\Delta r^2} \right) - r_O. \end{aligned} \quad (\text{A7})$$

References

- Brighton CT, Heppenstall RB. 1971. Oxygen tension in zones of the epiphyseal plate, the metaphysis and diaphysis. An in vitro and in vivo study in rats and rabbits. *J Bone Joint Surg Am* 53:719–728.
- Brighton CT, Heppenstall RB, Labosky DA. 1971. An oxygen micro-electrode suitable for cartilage and cancellous bone. *Clin Orthop* 80: 161–166.
- Carver SE, Heath CA. 1999. Influence of intermittent pressure, fluid flow, and mixing on the regenerative properties of articular chondrocytes. *Biotechnol Bioeng* 65:274–281.
- Chu CR, Coutts RD, Yoshioka M, Harwood FL, Monosov AZ, Amiel D. 1995. Articular cartilage repair using allogeneic perichondrocyte-seeded biodegradable porous polylactic acid (PLA): a tissue engineering study. *J Biomed Mater Res* 29:1147–1154.
- Clark LC, Wolf R, Granger D, Taylor A. 1953. Continuous recording of blood oxygen tension by polarography. *J Appl Physiol* 6:189–193.
- Crank J. 1975. *The mathematics of diffusion*. Oxford, England: Clarendon Press.
- Dom C, Schunke M, Christesen K, Kurz B. 2002. Redifferentiation of dedifferentiated bovine articular chondrocytes in alginate culture under low oxygen tension. *Osteoarthritis Cartilage* 10:13–22.
- Du C, Klasens P, Haan RE, Bezemer J, Cui FZ, de Groot K, Layrolle P. 2002. Biomimetic calcium phosphate coatings on PolyActive 1000/70/30. *J Biomed Mater Res* 59:535–546.
- Falchuk KH, Goetzl EJ, Kulka JP. 1970. Respiratory gases of synovial fluids. An approach to synovial tissue circulatory-metabolic imbalance in rheumatoid arthritis. *Am J Med* 49:223–231.
- Freed LE, Hollander AP, Martin I, Barry JR, Langer R, Vunjak-Novakovic G. 1998. Chondrogenesis in a cell-polymer-bioreactor system. *Exp Cell Res* 240:58–65.
- Freed LE, Langer R, Martin I, Pellis NR, Vunjak-Novakovic G. 1997. Tissue engineering of cartilage in space. *Proc Natl Acad Sci USA* 94: 13885–13890.
- Glenister TW. 1976. An embryological view of cartilage. *J Anat* 122: 323–330.
- Grimshaw MJ, Mason RM. 2000. Bovine articular chondrocyte function in vitro depends upon oxygen tension. *Osteoarthritis Cartilage* 8: 386–392.
- Haselgrove JC, Shapiro IM, Silverton SF. 1993. Computer modeling of the oxygen supply and demand of cells of the avian growth cartilage. *Am J Physiol* 265:C497–C506.
- Hunziker EB, Quinn TM, Hauselmann HJ. 2002. Quantitative structural organisation of normal adult human articular cartilage. *Osteoarthritis Cartilage* 10:564–572.
- Kellner K, Liebsch G, Klimant I, Wolfbeis OS, Blunk T, Schulz MB, Gopferich A. 2002. Determination of oxygen gradients in engineered tissue using a fluorescent sensor. *Biotechnol Bioeng* 80:73–83.
- Lane JM, Brighton CT, Menkowitz BJ. 1977. Anaerobic and aerobic metabolism in articular cartilage. *J Rheumatol* 4:334–342.
- Lund-Olesen K. 1970. Oxygen tension in synovial fluids. *Arthritis Rheum* 13:769–776.
- Malda J. 2003. *Cartilage tissue engineering. The relevance of oxygen*. Thesis University of Twente, Enschede, The Netherlands.
- Maroudas A. 1970. Distribution and diffusion of solutes in articular cartilage. *Biophys J* 10:365–379.
- McKibbin B, Holdsworth FW. 1966. The nutrition of immature joint cartilage in the lamb. *J Bone Joint Surg Br* 48:793–803.
- Murphy CL, Sambanis A. 2001a. Effect of oxygen tension and alginate encapsulation on restoration of the differentiated phenotype of passaged chondrocytes. *Tissue Eng* 7:791–803.
- Murphy CL, Sambanis A. 2001b. Effect of oxygen tension on chondrocyte extracellular matrix accumulation. *Connect Tissue Res* 42:87–92.
- Nehring D, Adamietz P, Meenen NM, Pörtner R. 1999. Perfusion cultures and modeling of oxygen uptake with three-dimensional chondrocyte pellets. *Biotech Tech* 13:701–706.
- Obradovic B, Carrier RL, Vunjak-Novakovic G, Freed LE. 1999. Gas exchange is essential for bioreactor cultivation of tissue engineered cartilage. *Biotechnol Bioeng* 63:197–205.
- Obradovic B, Meldon JH, Freed LE, Vunjak-Novakovic G. 2000. Glycosaminoglycan deposition in engineered cartilage: experiments and mathematical model. *AIChE J* 46:1860–1871.
- O'Driscoll SW. 1999. Articular cartilage regeneration using periosteum. *Clin Orthop* 367(Suppl):S186–S203.
- O'Driscoll SW, Fitzsimmons JS, Comisso CN. 1997. Role of oxygen tension during cartilage formation by periosteum. *J Orthop Res* 15: 682–687.
- Oostra J, le Comte EP, van den Heuvel JC, Tramper J, Rinzema A. 2001. Intra-particle oxygen diffusion limitation in solid-state fermentation. *Biotechnol Bioeng* 75:13–24.
- Papadaki M, Mahmood T, Gupta P, Claase MB, Grijpma DW, Riesle J, van Blitterswijk CA, Langer R. 2001. The different behaviors of skeletal muscle cells and chondrocytes on PEGT/PBT block copolymers are related to the surface properties of the substrate. *J Biomed Mater Res* 54:47–58.
- Rahardjo YS, Weber FJ, le Comte EP, Tramper J, Rinzema A. 2002. Contribution of aerial hyphae of *Aspergillus oryzae* to respiration in

- a model solid-state fermentation system. *Biotechnol Bioeng* 78: 539–544.
- Revsbech NP, Ward MW. 1983. Oxygen microelectrode that is insensitive to medium chemical composition: use in an acid microbial mat dominated by *Cyanidium caldarium*. *Appl Environ Microbiol* 45:755–759.
- Silver IA. 1975. Measurement of pH and ionic composition of pericellular sites. *Phil Trans R Soc London B Biol Sci* 271:261–272.
- Smith RL, Donlon BS, Gupta MK, Mohtai M, Das P, Carter DR, Cook J, Gibbons G, Hutchinson N, Schurman DJ. 1995. Effects of fluid-induced shear on articular chondrocyte morphology and metabolism in vitro. *J Orthop Res* 13:824–831.
- Smith RL, Trindade MC, Ikenoue T, Mohtai M, Das P, Carter DR, Goodman SB, Schurman DJ. 2000. Effects of shear stress on articular chondrocyte metabolism. *Biorheology* 37:95–107.
- Stockwell RA. 1979. *Biology of cartilage cells*. Cambridge, England: Cambridge University Press.
- Treuhart PS, McCarty DJ. 1971. Synovial fluid pH, lactate, oxygen and carbon dioxide partial pressure in various joint diseases. *Arthritis Rheum* 14:475–484.
- van Osch GJ, van der Veen SW, Buma P, Verwoerd-Verhoef HL. 1998. Effect of transforming growth factor- β on proteoglycan synthesis by chondrocytes in relation to differentiation stage and the presence of pericellular matrix. *Matrix Biol* 17:413–424.
- Vunjak-Novakovic G, Obradovic B, Martin I, Bursac PM, Langer R, Freed LE. 1998. Dynamic cell seeding of polymer scaffolds for cartilage tissue engineering. *Biotechnol Prog* 14:193–202.
- Woodfield TBF, Bezemer JM, Pieper JS, van Blitterswijk CA, Riesle J. 2002. Scaffolds for tissue engineering of cartilage. *Crit Rev Eukaryot Gene Expr* 12:207–235.
- Ye GF, Silverton SF. 1994. Computer-modeling of oxygen supply to cartilage: addition of a compartmental model. *Adv Exp Med Biol* 361:31–39.
- Zipper H, Papierman SK, Libbin RM, Person P. 1981. Development of chick limb bud chondrocytes in cell culture: morphologic and oxidative metabolic observations. *Clin Orthop* 155:186–195.